Studies on geosynthetic-reinforced road pavement structures

K. Rajagopal, S. Chandramouli, Anusha Parayil & K. Iniyan

Studies on geosynthetic-reinforced road pavement structures

K. Rajagopal*, S. Chandramouli, Anusha Parayil and K. Iniyan

Many of the pavement structures fail well before their design life owing to the poor quality of construction materials, inadequate compaction, inadequate preparation of the subgrade, over-loading, etc. Two options are available to improve the longevity of the pavement. The first option is by increasing the thickness of different pavement layers and the other option is by increasing the rigidity of the layers within the system so as to reduce the stresses transferred to the lower layers. Of these two methods it has been widely observed that increasing the strength and rigidity of the pavement layers is a more efficient method to lower the stresses on the pavement layers thereby increasing the life of the pavement.

In the present research work, the improvement in the strength and stiffness of the subbase layer in a flexible pavement system through the use of geosynthetic layers was investigated by conducting field plate load tests and a series of laboratory plate load tests. The improvement in the strength of the pavement is reflected by the increase in modulus of the section reinforced with geosynthetic layers. This paper will describe the field and laboratory tests, interpretation of the data from these tests, and the application of this data for design of flexible pavements and their economic analyses.

This paper is part of a special issue on geosynthetics

Introduction

The performance of highway pavements is governed by the strength and stiffness of the pavement layers. The cost and duration of construction are dependent on the availability of aggregate materials for construction. Scarcity of natural resources often delays the projects or escalates the costs due to large lead distances from the borrow areas. Hence, it is essential to look at alternatives to achieve improved quality of pavements using new materials and reduced usage of natural materials, Giroud and Han (2004). This paper reports on the studies of the performance of geosynthetic-reinforced flexible pavements. Different types of geosynthetics like planar (geogrids and geotextiles) and three dimensional (geocells) can be employed for strengthening the pavement bases. The geocells are three-dimensional honeycomb geosynthetic products that provide all round confinement to the soils. The geocell-confined soil acts like a semi-rigid mat in distributing the surface loads over a wide area of the foundation soil.

The performance of the geocells as surface confinement layers and as reinforcement layers has been reported by several researchers in the past. Bathurst and Rajagopal (1993) and Rajagopal *et al.* (1999) have reported the strength and stiffness behavior of soils confined in single geocell and multiple geocell pockets. Madhavi Latha *et al.* (2008, 2009) have reported the benefit of using geocells as basal reinforcement layers for embankments constructed on soft foundation soils. It was reported that the factor of safety of the slopes can be increased significantly because of the interception of the slip surface by the geocell layer. Unni (2010) and Chandramouli (2011) have reported the construction of geocell-reinforced unpaved road pavements and their performance on different types of subgrade layers. Iniyan (2012) has reported the use of geogrids for construction of pavements and the improvement of the strength of the pavement sections. Based on the higher modulus obtained with geosynthetic reinforcement layers, he has discussed that the pavement thickness can be reduced while maintaining the same level of design parameters.

Geocells and geosynthetics are adopted in several road and ground stabilization projects across the globe. Han *et al.* (2008, 2010, 2011) have described the influence of the infill material and the stiffness on the performance of geocells in pavements. Unni (2010), Chandramouli (2011),

Department of Civil Engineering, IIT Madras, Chennai 600 036, India

*Corresponding author, email gopalkr@iitm.ac.in

Iniyan (2012), and Parayil (2013) have reported the performance of geosynthetic-reinforced flexible pavement sections. They reported that the stresses below the reinforced layers are two to three times lesser than the surface stresses. Emersleben and Meyer (2010) conducted test box analysis for 200 mm height geocell filled with sand above very soft clay and observed that the stresses can be reduced by 30 and 36% depending on the applied load. The load carrying capacity could be improved up to 1·5 times due to the reinforcement of dry sand with geocells. Shin *et al.* (2010) conducted field plate load tests on reinforced and unreinforced subgrade soil and analyzed by using finite element software. They gave the subgrade improvement factor of 2. Bush *et al.* (1990) carried out research on geocell-reinforced embankment and concluded that the 1 m high geocell with local soil infill will have 33% lesser settlements after 4 years when compared to systems with horizontal layers of reinforcement. Further, the cost savings of more than 31% were reported for geocell-treated constructions.

The current paper investigates the performance of the reinforced flexible pavements under monotonic and repeated loads. The granular subbase and sand materials were obtained from a highway construction site near Chennai. All the index tests were performed to characterize these materials. Field and laboratory plate load tests were conducted on the flexible pavements. The pressure–settlement data was used to back-calculate the elastic modulus of the geosynthetic-reinforced pavement layers.

Field studies on geosynthetic flexible pavements

Geocell-reinforced pavements

The internal access roads at Govind Dairy Factory in Phaltan, Maharashtra required frequent repairs. The foundation soil is typically black cotton soil, which undergoes severe swelling and shrinking. The properties of this soil are given in Table 1. The roads are typical unpaved roads with thick layers of water-bound Macadam (WBM) and granular subbase (GSB) materials. Nearly 200 m long stretch of this road was treated with 150 mm thick geocell layer on an experimental basis to study the performance improvement.

Based on the soil properties and the traffic data, the following designed section of pavement as shown in Fig. 1 was used for reconstructing the road using geocell reinforcement. The geocell pockets were filled with GSB materials. Water-bound Macadam layers were not used within this stretch of road where geocell was used as a reinforcement layer. The bottom most layer was treated with 4% lime (hydrated lime) in order to stabilize the expansive foundation soil. Addition of 3% lime itself was found to reduce the plasticity index substantially. Hence, slightly higher percentage of 4% lime addition was recommended in order to account for any losses during installation and service life.

The geocell is 150 mm high and made of a polymeric alloy. The thickness of the geocell walls is approximately 1·2 mm. The c/c weld distance is 330 mm and the pocket
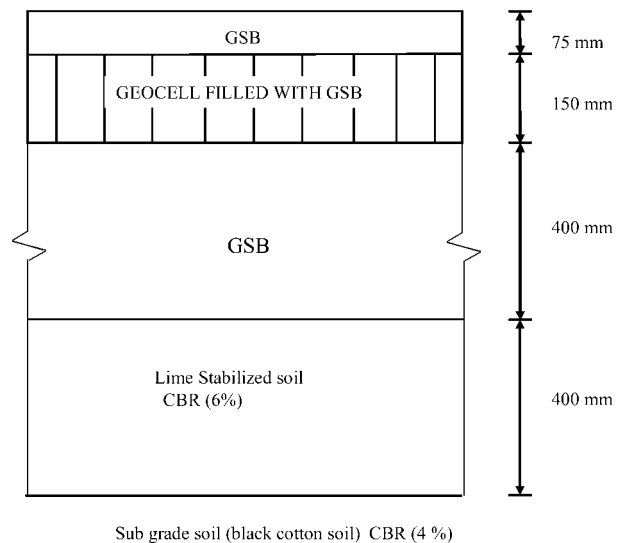
1 Cross-section of the pavement section at Govind Dairy Factory

opening dimensions are approximately 210×250 mm. The tensile strength of the geocell material in strip tension test was found to be 0·25 kN (ASTM D638-2003) and the peel strength of the weld is 0·2 kN from ASTM D6392-99 standard tensile strength tests. There was no change of dimensions when pieces of the geocell were exposed to 100°C temperature in an oven for 1 h duration (ASTM D1204).

The construction at the site proceeded by excavating the soil to the required depth. The hydrated lime was spread on the soil and mixed by a tractor with a plow attachment. The lime was mixed in proportion of 4% by weight. This percentage was decided based on prior experience with similar soils in India. The addition of 3% lime was found to drastically reduce the plasticity index values by as much as 50%. Hence, 4% lime mixing was recommended to account for some loss during and after the construction. After the compaction of the lime-treated soil and the granular subbase layers were completed, the geocell layer was spread on the road section and held in place by use of stakes driven into ground at 485 mm c/c spacing. The geocell pockets were filled with GSB material by a tipper truck and spread using a dozer. Care was taken to make sure that the vehicles do not pass directly on unfilled geocell section. After the geocell pockets were filled with GSB material and 75 mm cover material was placed, the entire section was compacted using normal 10-ton vibro roller passes. The photographs in Figs. 2–5 illustrate the construction procedure adopted at the site.

Table 1 Properties of subgrade soil

California bearing ratio (CBR)	4%
Swell index	150%
Liquid limit	60%
Plastic limit	25%
Shrinkage limit	8%

2 Mixing of the lime by a tractor

5 Compaction by a vibratory roller

3 Geocell layer spread over the road section

The construction of the pavement took place in March 2010. The unreinforced pavement sections were also constructed in the same manner without the geocell reinforcement at the subbase level. This stretch of road was provided with layers of WBM material, which is more expensive compared to GSB material. In place of the 400 mm thick GSB layer, two layers of 200 mm thick WBM layers were provided. Over this 150 mm thick layer of GSB was provided. The thickness of the lime-treated soil is the same as shown in Fig. 1.

The performance of the geocell-reinforced pavement and the adjacent unreinforced sections were monitored for their performance. The year 2010 was characterized by unusually heavy rainfall in that region. The unreinforced pavement had undergone severe rutting and had to be reconstructed at least three times by dumping of aggregate and recompaction during the period March–December 2010. The photographs of the unreinforced and the

4 Filling the geocell pockets with a dozer

6 Settlements observed in the unreinforced section

7   Uniform surface observed in the geocell section

reinforced pavement sections after 9 months of traffic loading are shown in Figs. 6–7 for comparison purposes.

The unreinforced pavement section had undergone severe surface depressions as indicated by the arrows. On the other hand, the geocell-reinforced road section had maintained a uniform surface. The trucks had to negotiate the unreinforced sections at a slow speed while they could maintain their normal speed in the reinforced sections. This difference in the performance clearly shows the improvement in the performance of the flexible pavements with geocell reinforcement. The performance of the geocell-treated section is very good even 3 years after its installation in 2010. The client has decided to reconstruct the entire stretch of their internal roads using geocell reinforcement.

In order to differentiate the strength of the pavement sections, plate load tests were performed at the site as per

IS 1888–1988 in the geocell-treated area and the unreinforced areas. Two tests were performed in geocell-reinforced area (R-1 and R-2) and two tests were performed in unreinforced pavement area (UR-1 and UR-2). One test was performed at subgrade level for comparative purposes. All the tests were performed at surface level after scraping the top 50 mm of pavement material. The observed pressure–settlement responses are shown in Fig. 8. The pressure–settlement responses of both the tests performed in geocell-treated pavement were very close to each other. The responses from the unreinforced areas are also very similar. The unreinforced pavement area was repaired several times by dumping large size stones, which are in excess of 200–300 mm in size. The test plate may have been located inadvertently over a large size stone in UR-2, which gave a stiffer response than the tests performed in geocell-treated area.

Geogrid-reinforced pavements

Two sections of a highway under construction near Chennai were reinforced with two different types of geogrids (flexible and stiff). Both geogrids are biaxial type having tensile strengths in the same range. The flexible geogrid was a knitted polyester geogrid having tensile strength of 100 kN m^{-1} at a strain of 10%. The stiff geogrid was an extruded and welded polyester geogrid, which is much heavier and stiffer. The stiff geogrid had a tensile strength of nearly 130 kN m^{-1} at a strain of 6%. The geogrid layers were placed within the subbase layer of the pavement at a depth of 200 mm below the surface. These two trial stretches were constructed next to each other so that the subgrade soil is similar. The subgrade soil at this site has a soaked CBR value of 8%. The pressure–settlement data of test performed at subgrade level is also shown for comparison. Two tests were performed on top of 200 mm thick granular subbase material without any
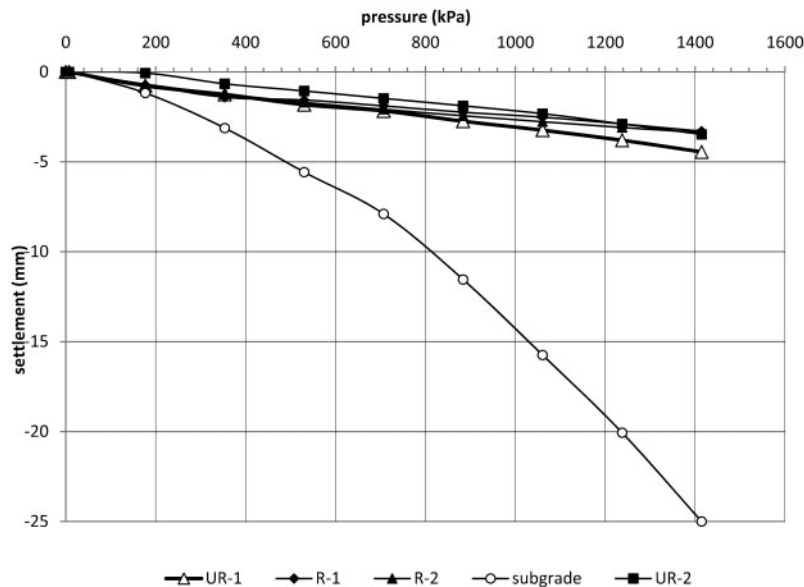
8   Pressure–settlement response from different field plate load tests
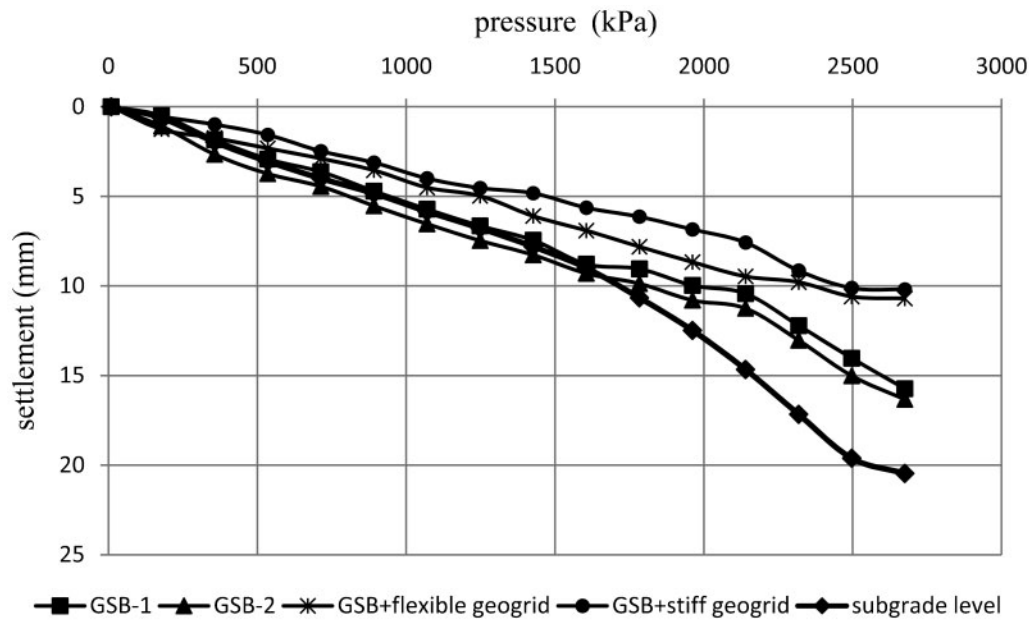
9 Pressure–settlement response with two different types of geogrids

geogrid reinforcement and one plate load test was performed within each of the two different types of geogrids. The observed pressure–settlement data is shown in Fig. 9. It could be seen that the response with the geogrid layers is stronger compared to the unreinforced sections. The observed pressures with stiffer geogrid are higher than those with flexible geogrid owing to the higher modulus of the stiff geogrid.

Discussion on field test results

It is interesting to note the following points from the field test results (Figs. 8 and 9):
1. The improvement of the response with geogrid reinforcement layers is practically nil at low settlement levels.
2. The marginal improvement with geogrid layers is seen only at large settlement levels.
3. The improvement with geocell reinforcement is substantial even at low settlements.
4. The improvement at large settlements is substantial with geocell reinforcement.

Laboratory studies

The laboratory plate load tests were performed under monotonic and cyclic conditions to examine the benefit of the reinforcement layers under repeated loadings. The laboratory tests were performed in a rigid steel tank having plan dimensions of 1200×1200 mm and height of 1200 mm. The steel tank was made of 8 mm thick steel plate and supported around its periphery by a frame made of 75 mm L-angles. The diameter of the plate used for loading was 150 mm and the thickness was 30 mm. The load was applied to the plate through a hydraulic jack fixed against a rigid self-reacting frame.

All the tests were performed by constructing 500 mm thick subgrade made up of dry sand placed at 60% relative density. The sand is uniformly graded coarse sand with angular particles having the properties listed in Table 2. The sand was placed at 60% relative density in all the tests. It was closely monitored in all the tests by collecting soil

Table 3 Properties of the granular subbase (GSB) material

Material type		GSB (granular subbase)
Dry density		$2 \cdot 19$ g cc^{-1}
Optimum moisture content		$5 \cdot 31$%
CBR value in loose state		23%
Particle size distribution	>4·75 mm	71·6%
	4·75–2·36 mm	5·2%
	2·36–0·075 mm	18·5%
	<0·075 mm	4·7%
Shear strength properties		$c=0$, $\phi=65°$

Table 2 Properties of sand used in the laboratory tests

Specific gravity	Effective size (D_{10})/mm	Coefficient of uniformity C_u	Coefficient of curvature C_c	Maximum unit weight/kN m^{-3}	Minimum unit weight/kN m^{-3}	Friction angle/°
2·66	0·55	2·9	1·6	16·1	14·5	46°
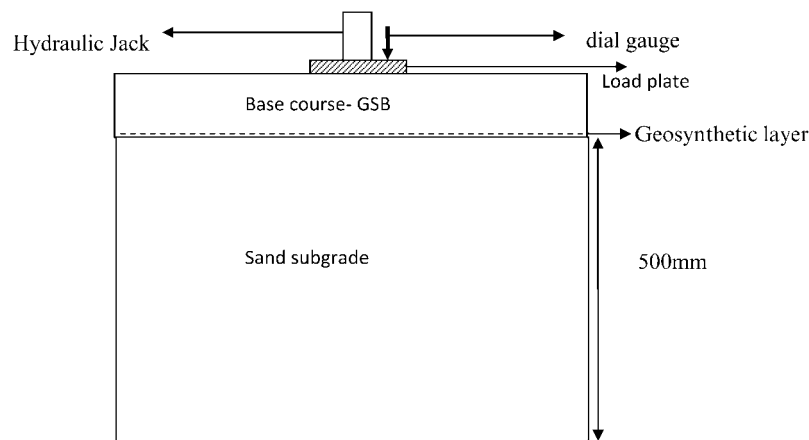
10 Schematic of the load testing in laboratory

samples using steel containers buried in the soil at different depths.

The base course was constructed using GSB material of coarse particles having the properties listed in Table 3. The GSB was placed in the test tank in a relatively loose state by hand packing. The laboratory CBR value for this packing was nearly 23%.

The base layers were reinforced with geocell or geogrid layers. In all the tests, the sand and GSB material were separated by a woven geotextile layer. The properties of different geosynthetic materials are listed tables 4 and 5. Three different heights of geocell layers 50, 100, and 150 mm were used in this testing program.

The geogrid used is a polyester knitted type geogrid having the properties listed in Table 5. The tensile properties of the geogrid layer were determined as per ASTM D 6647-11. The strain corresponding to the ultimate strength is 10%. The same geocell used for field tests was also used in the laboratory tests.

The total thickness of the subgrade of 500 mm was prepared in four layers of thickness 150, 150, 100, and 100 mm. The quantity of the sand required in each layer was pre-weighed and placed in layers with light compaction to achieve 60% relative density of the soil. The relative density achieved was carefully monitored by placing steel cups of known volume and collecting soil samples after each layer of compaction.

The geosynthetic reinforcement (geotextile, geogrid, or geocell) was placed on the prepared subgrade. While placing the geocell, each pocket was stretched to at least 180 mm size and the corners were filled with aggregate to keep it in position. Then the other pockets of the geocell were carefully filled with GSB by hand packing. In case of geocell an additional 10 mm of GSB was provided over the weld to prevent direct load application on to the geocell.

The schematic representation of testing is shown in Fig. 10. The settlements were measured using electronic linear voltage differential transducers (LVDTs) and the load was measured using an electronic load cell. The load was applied in small increments. The load increment was maintained constant until the settlements under that increment cease to increase. Then the next increment of load was applied. Since the subgrade is sand, settlements have become constant within 1 min of load application. The test was terminated when the base could not continue to hold any further load increment.

Table 4 Properties of geotextile layer used in the laboratory tests

Geotextile type	Mass per unit area/g m^{-2}	Nominal thickness/mm	Ultimate tensile strength/kN m^{-1}	Maximum Elongation/%
Woven	240	0·5	115	14

Table 5 Properties of geogrid used in the tests

Mass per unit area/g m^{-2}	Nominal thickness/mm		Ultimate tensile strength/kN m^{-1}	
	MD	CD	MD	CD
918	2·1	1·67	110	23

MD: machine direction; CD: cross-machine direction.
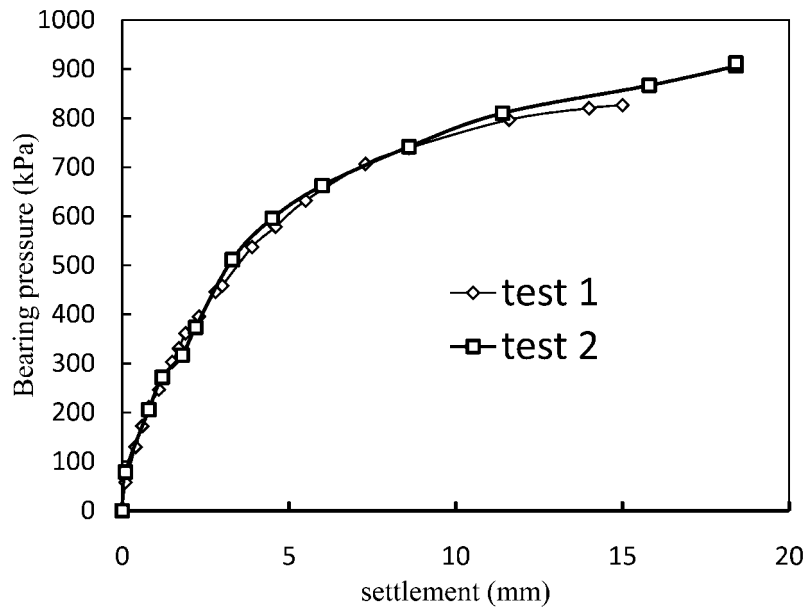
11 Pressure–settlement data from two tests performed on 100 mm thick granular subbase (GSB) layer

The consistency of the test results is very important when results from different tests are to be compared. Several trials were made initially until achieving consistent pressure–settlement data. Typical pressure–settlement data from two different tests with the same configuration is shown in Fig. 11. It could be seen that the two pressure–settlement responses are almost identical. Hence, it could be concluded that the results from this testing program are repeatable. Typical pressure–settlement responses for 150 mm thick GSB layer and different forms of geosynthetic reinforcement are illustrated in Fig. 12. From the

measured pressure–settlement data, the ultimate bearing capacities for different test configurations are obtained as shown in Table 6. The ultimate pressures were obtained by drawing tangent lines to the initial and the final parts of the pressure–settlement responses. The ultimate pressure is given by the intersection point of these two tangent lines as illustrated in Fig. 12.

After each test was completed, the GSB layer was carefully removed to examine the settlement bowl at the surface of the subgrade. After the subgrade was exposed, the radial extent of the settlement bowl and the settlements
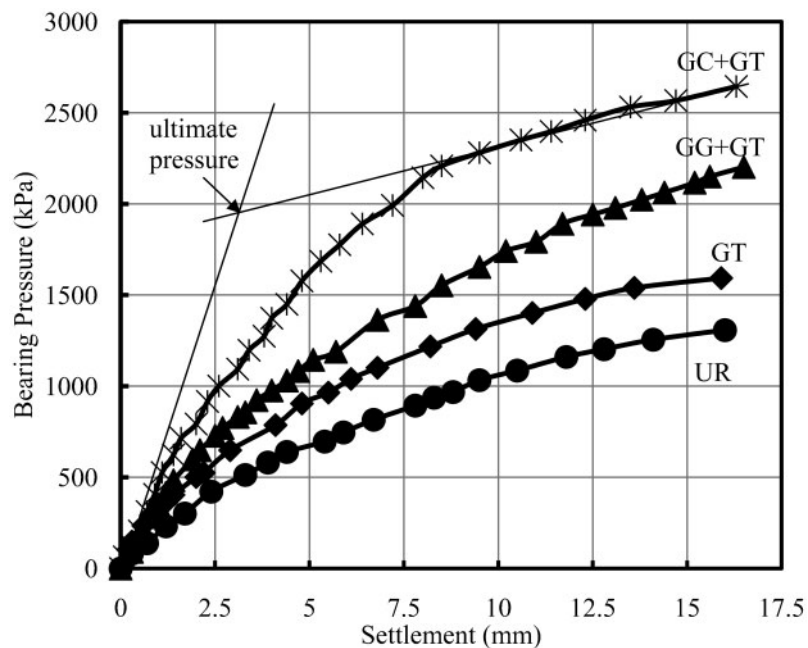
12 Pressure–settlement response with different types of reinforcements for 150 mm thick granular subbase (GSB) base layer: UR: unreinforced; GT: geotextile; GG + GT: geogrid + geotextile; GC + GT: geocell + geotextile
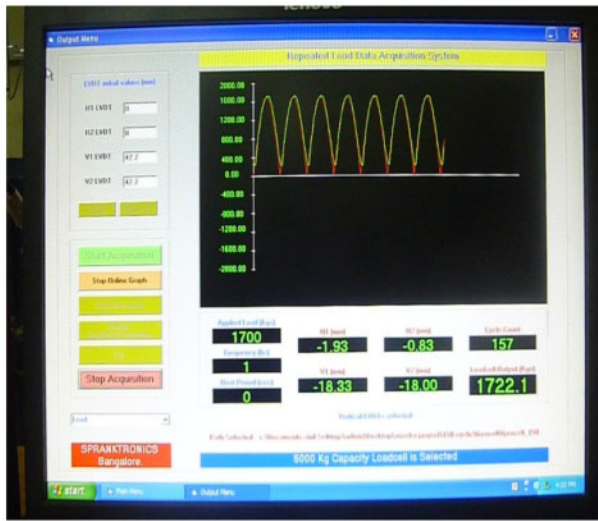
13 Screen shot of the computer screen during cyclic load tests

within the bowl were carefully measured. In general, it was noticed that the loads are distributed over a larger area of the subgrade due to the provision of the geosynthetic layer. The tests were performed with a single layer of geotextile, combination of geotextile and geogrid, and a geocell underlain by a geotextile, which acts as a separator layer. The ratio between the diameters of the settlement bowl and the loading plate gives an idea of the pressures transmitted to the subgrade. These ratios for different test configurations are given in Table 7.

It is seen that for geosynthetic-reinforced cases, the diameter of the settlement bowl is much bigger leading to lesser pressures transmitted to the subgrade soil. The settlement bowl for the geocell reinforcement is found to be biggest among all the reinforced cases.

The pavements are subjected to number of load repetitions during their service life. The response of the pavements under repeated loading may be much different from that under static loading. Hence, several tests were performed by subjecting the pavement sections to repeated loading (cyclic loading). The loading was applied as one-way cyclic loading. The load was increased to a pre-set maximum value and reduced to a lower value (1 kN) and increased once again. The same configurations used for static load tests were also used for the cyclic plate load tests.

The maximum load in the cyclic load tests was decided based on the ultimate bearing pressure observed in the static load tests. The pavement section was prepared in the same manner as in the monotonic plate load test. After the section is set up, two dial gages were fixed on top of the load plate. The cyclic loading was applied through a servo-controlled hydraulic actuator. The system is operated using a computer program that acquires the load and deformation data. The cyclic loading was applied at a frequency of 0·7 Hz for 50 000 cycles. This loading frequency was reported by Pokharel *et al.* (2010) and Han *et al.* (2011) as that representative of the traffic loading. The pressures applied in these tests are the ultimate pressures observed for respective thickness of the unreinforced sections viz. 610, 725, and 930 kPa for 50, 100, and 150 mm thick GSB layers, respectively.

**Table 6   Ultimate bearing pressures for different test configurations**

Base course thickness/mm	Ultimate bearing capacity/kPa			
	Unreinforced	Geotextile	Geogrid+geotextile	Geocell+geotextile
50	610	630	920	1560
100	725	1320	1510	1980
150	930	1370	1530	2045

Table 7   Ratio of the diameter of settlement bowl and the loading plate

Thickness of base layer/mm	Unreinforced	Geotextile	Geogrid+geotextile	Geocell+geotextile
50	2·15	2·2	2·25	2·43
100	2·33	2·53	2·59	2·77
150	2·56	2·62	2·74	2·87

Table 8   Maximum settlements at the end of 50 000 load cycles

Thickness of base course/mm	Applied pressure/kPa	Maximum settlement/mm			
		Unreinforced	Geotextile	Geogrid+geotextile	Geocell+geotextile
50	610	23·17	14·48	10·49	8·08
100	725	39·18	24·5	19·88	15·2
150	930	46·12	28·61	24·6	20·9
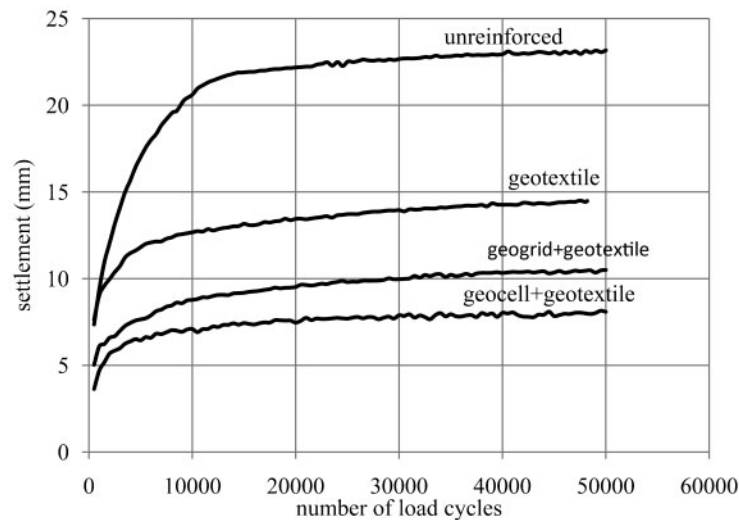
14 Variation of settlement with number of load repetitions

A screen shot of the cyclic loading program is shown in Fig. 13. The green line shows the load calculated as per the applied load and the red line shows the load measured by the load cell in the actuator. It is seen that both are very close to each other.

Typical data on the variation of settlement with different types of geosynthetic reinforcement layers for 50 mm thick GSB layer are shown in Table 8 and Fig. 14.

From the above measured data, the modulus of subgrade reaction can be estimated as the ratio of the applied pressure, the base area, and the settlement.

Knowing the values of the applied load P, radius of the loading plate a, and the settlement s, the modulus of subgrade reaction can be calculated from the data as

$$M = \frac{P}{\pi \, a^2 \, s} \tag{1}$$

The results showed that initially the modulus of the subgrade is very high and as the settlement increased with number of cycles, the modulus value decreased and reached a constant value toward the end of 20 000 cycles.
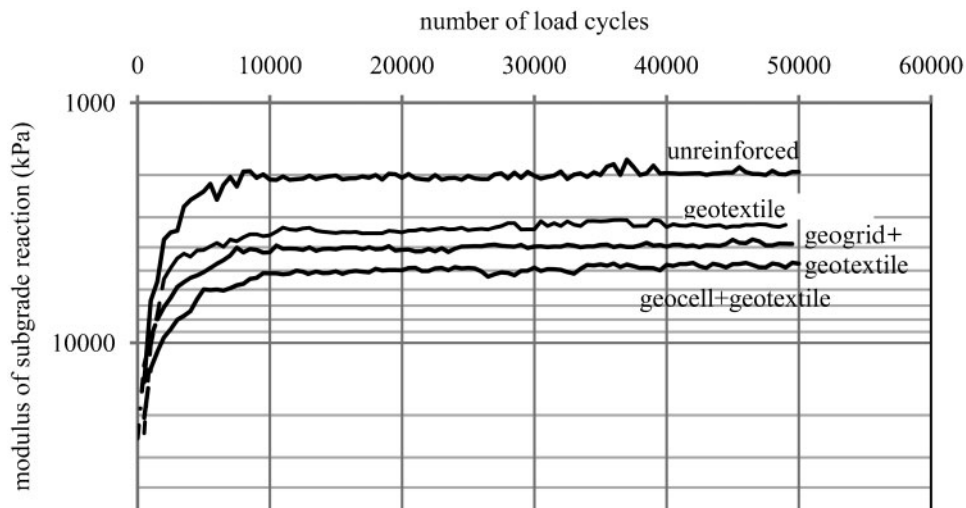
15 Variation of the modulus of subgrade reaction with number of load cycles

Table 9 Modulus of subgrade reaction obtained at the end of 50 000 cycles

Modulus of subgrade reaction/kN m^{-3} Thickness of base course/mm	Unreinforced	Geotextile	Geogrid + geotextile	Geocell + geotextile
50	3011	4813	5802	7031
100	1941	3224	3866	4650
150	1861	3150	3868	4489
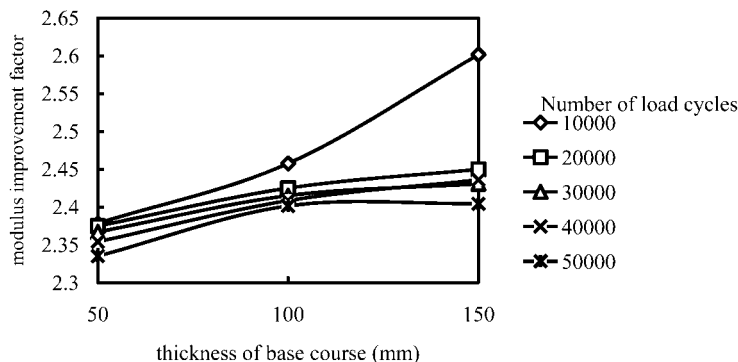
16 Variation of modulus improve factor with the number of cycles for geocell case

The typical variation of the subgrade modulus with different number of cycles is shown in Fig. 15 for 100 mm thick GSB layer.

The modulus values obtained at the end of 50 000 cycles are shown in Table 9.The geosynthetic reinforcement improved the modulus of subgrade reaction of the test section for all thicknesses of the base course layer. The reduction in modulus value with increased base layer thickness is due to the compressions within the base layer as it was placed in loose state.

The modulus improvement factor is defined as the ratio of elastic modulus of the reinforced base course to that of unreinforced base course of the same thickness. The modulus of subgrade reaction values at the end of 50 000 cycles are used to calculate the modulus improvement factors for illustration purposes. The improvement factors thus obtained are given in Table 10. It can be seen that the

modulus improvement is higher for geocell-reinforced cases and its value is higher for larger heights of the base layers.

The modulus improvement factor was found to vary with the number of cycles. The modulus improvement factor was also found to be high initially and as the number of load cycles increased, the value was found to decrease as illustrated in Fig. 16. This decrease is mainly attributed to the loose state of the base layer, which has undergone compressions due to repeated load applications.

Back calculation of elastic modulus of the system

Elastic finite element analyses were performed to estimate the equivalent elastic modulus of the unreinforced and reinforced pavement systems. The finite element analyses

Table 10 Modulus improvement factors from cyclic plate load test data

	Thickness of base course/mm	Geotextile	Geogrid + geotextile	Geocell + geotextile
Modulus improvement factor	50	1·6	1·93	2·34
	100	1·67	1·99	2·40
	150	1·70	2·08	2·41

Table 11 Modulus of elasticity of granular subbase (GSB) from finite element analyses

	Modulus of elasticity/kPa			
Thickness/mm	Unreinforced	Geotextile	Geogrid + geotextile	Geocell + geotextile
50	25 500	44 100	52 000	70 500
100	29 100	50 500	61 100	84 500
150	33 000	58 000	74 000	98 000

Table 12 Modulus improvement factors from finite element results

	Improvement factors		
Thickness/mm	Geotextile	Geogrid + geotextile	Geocell + geotextile
50	1·73	2·04	2·76
100	1·74	2·10	2·90
150	1·76	2·24	2·97

were performed by using axi-symmetric model and 15-node triangular elements. The rough, rigid footing was simulated by applying uniform settlements at the nodes corresponding to the footing and restraining their lateral deformations.

The equivalent elastic modulus was determined by trial and error by matching the finite element calculated footing pressure at 1·5 mm settlement (equal to 1% of plate diameter) with the measured pressures in the laboratory tests. It is assumed that the response of the system at a small settlement equal to 1% of the footing diameter is within the elastic limit. The elastic modulus value of the continuum was varied until the estimated pressure matches with the experimentally measured values. The results of the monotonic plate load tests were used for these analyses. The elastic modulus values back calculated for different cases are listed in Table 11.

The modulus improvement factor for the reinforced cases is calculated as the ratio between the modulus of the reinforced system and the corresponding modulus of the unreinforced cases. These values are reported in Table 12. It is interesting to note that these improvement factors fall within the same range as those estimated using the cyclic load test results. Hence, it may be possible to utilize the results from static load tests for preliminary design purposes without incurring too much of an error. However, the designs will not be conservative as the modulus improvement factors from static load tests are about 15% higher than those from cyclic load tests.

The modulus improvement factors are required in mechanistic-based design of flexible pavements in which the modulus values of each pavement layers are to be given as input values, e.g. CIRCLY program for design of pavements. These modulus improvement factors can be used to represent the equivalent behavior of the geosynthetic-reinforced pavement sections. The use of higher modulus for the pavement layers results in lesser thickness for the layers as the pressure transmitted to the subgrade reduces with increase in the modulus values. By using different modulus improvement factors in the CIRCLY program, Iniyan (2012) has studied the influence of geocell and geogrid layers on the thickness of the pavement layers. Reduced thickness of the pavement layers results in lesser total cost of the pavement and lesser construction times. This will also lead to lesser carbon footprint as reduced quantities of natural aggregate materials are required for construction.

Conclusion

This paper has presented some results from field and laboratory tests on the performance of pavements with different types of geosynthetic reinforcements. It is seen that both the strength and stiffness of the pavement system can be improved by the use of geosynthetics. The performance under repeated loads is also better with geosynthetic reinforcement layers.

The improvement in the overall performance is by distributing the applied loads over a much wider area of the subgrade thus reducing the stresses at the subgrade level. The geocell reinforcement gives much higher improvement in the pavement performance as compared to the planar type products like geotextiles and geogrids.

The modulus improvement factors obtained from both monotonically applied tests and the cyclic load tests are close to each other. Significant improvement is observed for all types of geosynthetic reinforcement systems. The modulus improvement factor is seen to be higher for monotonic loading as compared to the cyclic load tests. This could be due to the loose packing of the GSB layer in laboratory tests leading to continuous compressions within the GSB layer under cyclic loading.

Ackowledgement

References

ASTM D 0638. 2003. Standard test method for tensile properties of plastics, West Conshohocken, PA, USA, ASTM International.

ASTM D1204. 2008. Linear dimensional changes of nonrigid thermo-plastic sheeting or film at elevated temperature, West Conshohocken, PA, USA, ASTM International.

ASTM D 6392. 2008. Determining the integrity of nonreinforced geomembrane seams produced using thermo-fusion methods, West Conshohocken, PA, USA, ASTM International.

ASTM D6647. 2001. Test method for determining tensile properties of geogrids by the single or multi-rib tensile method, West Conshohocken, PA, USA, ASTM International.

Bathurst, R. J. and Rajagopal, K. 1993. Large scale triaxial compression testing of geocell-reinforced granular soils, *Geotech. Test. J.*, **16**, 3, 296–303.

Bush, D. I., Jenner, C. G. and Bassett, R. H. 1990. The design and construction of geocell foundation mattresses supporting embankments over soft ground, *Geotext. Geomembr.*, **9**, 83–98.

Chandramouli, S. 2011. Performance and economic evaluation of geocells in the road pavement structure, Thesis submitted in partial fulfillment of the requirements of the MTech degree, Department of Civil Engineering, Indian Institute of Technology Madras, Chennai, India.

CIRCLY. 2013. Software for design of flexible pavements, Richmond, VIC, Australia, MINCAD Systems Pvt. Ltd.

Emersleben, A. and Meyer, N. 2010. The influence of hoop stresses and earth resistance on the reinforcement mechanism of single and multiple geocells, 9th International Conference on Geosynthetics, Brazilian Chapter of International Geosynthetics Society, IGC-2010, Guaruja, Brazil, May 23-27, 713–716.

Giroud, J. P. and Han, J. 2004. Design method for geogrid-reinforced unpaved roads. I. Development of design method and II. Calibration of applications, *J. Geotech. Geoenviron. Eng.*, **130**, (8), 775–797.

Han, J., Pokharel, S. K., Parsons, R. L., Leshchinsky, D. and Halahmi, I. 2010. Effect of infill material on the performance of geocell-reinforced bases, 9th Int. Conf. on 'Geosynthetics' (ICG 2010), Brazil, May 23–27.

Han, J., Pokharel, S. K., Parsons, R. L., Leshchinsky, D. and Halahmi, I. 2010. Effect of infill material on the performance of geocell-reinforced bases, 9th International Conference on Geosynthetics, Brazilian Chapter of International Geosynthetics Society ICG 2010, Guaraja, Brazil, May 23-27, 1503–1506.

Han, J., Yang, X. M., Leshchinsky, D. and Parsons, R. L. 2008. Behavior of geocell-reinforced sand under a vertical load, *J. Transp. Res. Board*, **2045**, 95–101.

Iniyan, K. 2012. Influence of geogrid reinforcement on the carbon footprint of flexible pavements, Thesis submitted in partial fulfillment of the requirements of the MTech degree, Department of Civil Engineering, Indian Institute of Technology Madras, Chennai, India.

IS 1888. 1988. Method of load test on soils, Bureau of Indian Standards, New Delhi.

Madhavi Latha, G., Dash, S. K. and Rajagopal, K. 2008. Equivalent continuum simulations of geocell reinforced sand beds supporting strip footings, *Geotech. Geol. Eng.*, **6**, (4), 387–398.

Madhavi Latha, G., Dash, S. K. and Rajagopal, K. 2009 Numerical simulation of the behaviour of geocell reinforced sand in foundations, *ASCE Int. J. Geomech.*, **9**, 143–152.

Parayil, A. 2013. Performance of geosynthetic reinforced flexible pavements, Thesis submitted in partial fulfillment of the requirements of the MTech degree, Department of Civil Engineering, Indian Institute of Technology Madras, Chennai, India.

Pokharel, S. K., Han, J., Leshchinsky, D., Parsons, R. I. and Halahmi, I. 2010. Investigation of factors influencing behavior of single geocell-reinforced based under static loading, *Geotext. Geomembr.*, **28**, 6, 570–578.

Rajagopal, K., Krishnaswamy, N. R. and Madhavi Latha, G. 1999. Behavior of sand confined with single and multiple geocells, *Geotext. Geomembr.*, **17**, 3, 171–184.

Shin, E. C., Kim, S. H. and Oh, Y. I. 2010. Comparison of bearing capacity on geocell-reinforced subgrade, *9th International Conference on Geosynthetics*, Brazilian Chapter of International Geosynthetics Society, IGC-2010, Guaruja, Brazil, May 23-27, 1441–1444.

Unni, A. 2010. Structural and economic evaluation of geocells in the road pavement structure, Thesis submitted in partial fulfillment of the requirements of the MTech degree, Department of Civil Engineering, Indian Institute of Technology Madras, Chennai, India.